Sulfonated Cellulosic Fabric Catalyst for Biodiesel Production from Waste Oils

Abstract

This work reports the synthesis of a bio-based acid catalyst derived from recycled cellulosic fabric, functionalized via sulfonic grafting, for the conversion of waste cooking oils into biodiesel. The resulting material exhibits a high acid density (1.31 mmol $H^{+} \cdot g^{-1}$) and a low pHpzc (~2.3), promoting substrate adsorption and protonation. Its catalytic performance was evaluated under various reaction conditions (70–120 °C, 5–20 wt% catalyst loading, methanol-to-oil molar ratios of 3:1–15:1). The best operating conditions (90 °C, 15 wt%, 9:1 ratio, and 10 h) yielded a FAME conversion of 97%, comparable to commercial resins.

The bifunctional catalysis enables single-step transformation of highly degraded oils (acid value 4.8 mg KOH/g, viscosity 42.3 mm^2/s), as confirmed by GC-MS (>95% conversion) and ^1H NMR (–OCH_3 peak at 3.7 ppm). The biodiesel produced meets EN 14214 and ASTM D6751 requirements, with a viscosity of 4.54 mm^2/s, density of 0.885 $g \cdot cm^{-3}$, and residual acid value of 0.38 mg KOH/g. The catalyst demonstrates good durability, with conversion decreasing from 97% to ~90% after five reuse cycles, confirming SO_3H site stability and its relevance for circular lipid valorization processes.

Keywords: Sulfonated cellulose; heterogeneous catalysis; waste oils; transesterification; biodiesel; catalytic durability.

1. Introduction

The increasing global demand for sustainable biofuels calls for the development of efficient, economical, and environmentally compliant catalytic solutions for converting renewable resources into biodiesel (Zhang & Li, 2022). Waste cooking oils, abundant in urban areas yet largely underutilized, offer strategic potential to lower production costs, reduce pressure on edible oils, and align with energy transition objectives (Mahmood et al., 2025). However, converting such degraded lipid matrices requires robust catalysts capable of operating effectively despite impurities, high acidity, and oxidative deterioration (Chen et al., 2024).

In this context, bio-derived heterogeneous catalysts are particularly attractive owing to their low cost, easy recovery, and compatibility with green chemistry principles (Li et al., 2021). Cellulose represents a promising support due to its availability, biodegradability, and modifiable hydroxyl functionalities enabling controlled introduction of catalytic sites (Klemm et al., 2020). The reuse of discarded cellulosic textiles further aligns with circular economy strategies, offering a low-cost and locally available substrate (Mahmood et al., 2025).

Among functionalization routes, cellulose sulfonation generates strong $–SO_3H$ proton sites that display high activity in esterification and transesterification, with acid densities above 1 mmol $H^{+} \cdot g^{-1}$ and catalytic yields exceeding 90% (Kaur et al., 2020; Zhou et al., 2023). This performance arises from a synergistic combination of accessible acidity, morphology reorganization induced by grafting, and enhanced diffusion of reactants toward active sites (Wang et al., 2022).

Despite these advances, the use of recycled cellulosic fabric as a catalytic platform for esterification and transesterification remains scarcely explored, although it represents a high-potential pathway for developing circular and low-carbon technologies (Mahmood et al., 2025). Current challenges include (i) controlling functionalization degree and acid density, (ii) understanding structure–acidity–activity relationships, (iii) assessing the influence of textural properties on intra-particle diffusion, and (iv) ensuring durability and recyclability under realistic operating conditions (Amarasekara, 2024).

In this context, the present work aims to develop a bio-based acid catalyst derived from recycled cellulose fabric, functionalized by sulfonic grafting, and to correlate its physicochemical properties with its catalytic performance during the conversion of waste cooking oils into biodiesel via transesterification.

2. Materials and Methods

2.1. Raw materials and reagents

The cellulosic support was obtained from locally collected 100% cotton textiles, in alignment with a circular economy approach. The fabrics were cleaned in two steps: washing with hot distilled water (70 °C) followed by ethanol extraction (95%) for 30 min under magnetic stirring, then oven-dried at 105 °C for 12 h. Analytical-grade reagents were used throughout: sodium metaperiodate ($NaIO_4$, ≥99%), chlorosulfonic acid ($ClSO_3H$, 98%), glacial acetic acid, methanol (99.8%), ethanol (99%), NaOH solutions (0.01–0.1 $mol \cdot L^{-1}$) for titration, and NaCl (0.01 $mol \cdot L^{-1}$) for pHpzc determination. Ultrapure water (18.2 MΩ·cm) was used in all synthesis, rinsing, and preparation steps.

2.2. Oxidative activation of the cellulosic support

Pre-oxidation was performed to generate reactive aldehyde groups. One hundred grams of dried textile were immersed in 1 L of $NaIO_4$ solution (0.1 $mol \cdot L^{-1}$) under magnetic stirring (300 rpm) for 6 h at 25 °C, protected from light to prevent periodate photoreduction. After reaction, the material was thoroughly washed with distilled water to neutrality, filtered, and dried at 105 °C for 12 h. Mass loss was used as an indicator of functional conversion.

2.3. Sulfonic grafting by chlorosulfonation

Acid functionalization was achieved by controlled introduction of $–SO_3H$ groups. Ten grams of oxidized cellulose (Cell–CHO) were dispersed in 100 mL of glacial acetic acid in a round-bottom flask equipped with a condenser and maintained under nitrogen. The suspension was cooled to 0–5 °C, after which chlorosulfonic acid was added dropwise (2 $mL \cdot g^{-1}$ of support) over 30 min. The mixture was then heated at 60 °C for 3 h. The resulting sulfonated material (Cell–SO_3H) was filtered, washed successively with acetone and distilled water to neutrality, and dried at 80 °C for 10 h. Grafting yield was calculated based on dry mass.

2.4. Physicochemical characterizations

2.4.1. Infrared spectroscopy (FT-IR)

FT-IR spectra were recorded in ATR mode (4000–400 cm^{-1}) with a resolution of 4 cm^{-1} to identify structural modifications (C=O, S=O, S–O).

2.4.2. Elemental analysis (CHNS)

Sulfur content was quantified by CHNS analysis and used to calculate theoretical acid density (mmol $H^+ \cdot g^{-1}$).

2.4.3. Total acidity determination

Acidity was measured by acid–base neutralization: 0.1 g of catalyst was suspended in 50 mL NaCl (0.01 $mol \cdot L^{-1}$) and titrated with NaOH (0.01 $mol \cdot L^{-1}$). Acid density was computed according to stoichiometric consumption.

2.4.4. pHpzc measurement (drift pH method)

A series of NaCl solutions (0.01 $mol \cdot L^{-1}$) with initial pH values ranging from 2 to 12 received 0.1 g of catalyst each. After 24 h equilibration, final pH values were recorded to determine the point of zero charge.

2.4.5. Scanning electron microscopy (SEM)

Fragments (~5 × 5 mm) of raw, oxidized, and sulfonated fabric were Au/Pd sputter-coated (~10 nm) and examined in secondary-electron mode (5–15 kV) to assess morphology and surface/textural evolution.

2.4.6. Thermogravimetric analysis (TGA/DTG)

Thermal stability was assessed using TGA/DTG between 30 and 600 °C under nitrogen (10 $°C \cdot min^{-1}$) to identify functional decomposition and support pyrolysis stages.

2.5. Transesterification catalytic tests

The catalytic activity of Cell–SO_3H was assessed for converting waste cooking oils into biodiesel. The oils were filtered (Whatman paper) to remove impurities and oven-dried at 105 °C for 1 h to lower residual moisture. In a refluxed round-bottom flask or temperature-controlled reactor, 100 mL of pretreated oil were mixed with methanol at molar ratios ranging 3:1–15:1. Catalyst loading was varied between 5 and 20 wt%. Reactions were conducted under stirring (600 rpm) at temperatures ranging 70–120 °C for 5–14 h, depending on the parameter studied.

After reaction, the catalyst was filtered, washed with methanol, and dried at 80 °C for reuse. The biodiesel phase was separated from glycerol, washed at 50–60 °C to neutrality, and dried at 105 °C.

Methyl ester (FAME) yields were determined by residual acid titration and confirmed by GC-MS, allowing correlation of catalytic performance with material structure and reaction conditions.

2.6. Catalyst reusability and stability

After reaction, the catalyst was recovered by filtration, washed with methanol, and dried at 80 °C for 4 h before reuse without further treatment. Stability was evaluated over successive cycles by monitoring conversion efficiency.

3. Results and Discussion

3.1. Chemical transformation of cellulosic fabric and acid functionalization

The conversion of recycled cellulosic textile into a heterogeneous acid catalyst proceeds through two major steps (Figure 1): selective periodate oxidation (formation of Cell–CHO) followed by sulfonic grafting (formation of Cell–SO_3H). The moderate mass loss observed after oxidation (~4.6%) reflects controlled cleavage of a fraction of vicinal diols, generating reactive aldehyde functions while preserving the integrity of the fibrillar matrix. This behavior aligns with recent studies on mild oxidative activation of cellulose for the introduction of acidic or chelating functionalities (Pandey et al., 2022).

Chlorosulfonic grafting leads to a high functionalization yield (~92.5%), suggesting strong affinity between activated surface groups and the sulfonating reagent. The acid density calculated from the sulfur content (3.8%) reaches ~1.25 mmol $H^+ \cdot g^{-1}$, in excellent agreement with the titrated value (1.31 mmol $H^+ \cdot g^{-1}$), indicating that most generated –SO_3H groups are accessible within the reaction medium. Such acid densities are comparable, or even superior, to those reported for biosourced sulfonated catalysts derived from carbon or lignocellulose materials, typically ranging between 0.8 and 1.3 mmol $H^+ \cdot g^{-1}$ (Kaur et al., 2020; Tsubaki et al., 2021; Zhou et al., 2023).

The consistency between theoretical and measured acidity confirms the reliability of the sulfonation protocol and represents an essential prerequisite for applications in waste oil

transesterification, which are highly sensitive to the availability and strength of protonic sites (Mahmood et al., 2025).

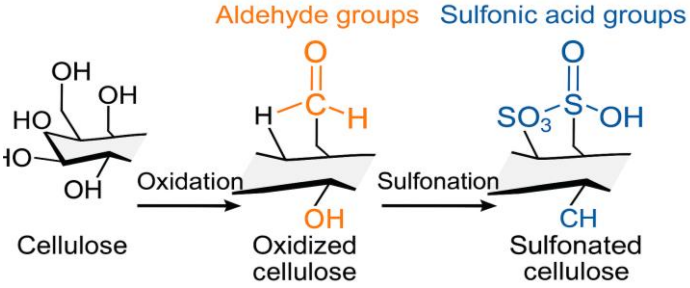

Figure 1. Schematic representation of the cellulose fabric functionalization process

3.2. Spectroscopic and structural confirmation of functionalization

Figure 2 (FT-IR spectra) clearly illustrates the structural evolution occurring throughout the successive modification stages of the cellulosic fabric. After oxidation, the emergence of a sharp band around 1720 cm^{-1}, assigned to aldehyde C=O stretching vibrations, confirms the formation of carbonyl functionalities from native diols. Following sulfonic grafting, new intense bands appear at ≈1180 and 1040 cm^{-1}, attributed respectively to S=O and S–O stretching modes of sulfonate groups (–SO_3H), validating the formation of Cell–SO_3H. The concomitant decrease in intensity of the broad 3330–3400 cm^{-1} O–H stretching band reflects partial substitution of hydroxyl groups by sulfonated functions, as previously reported for functionalized cellulose systems (Li et al., 2021; Wang et al., 2022).

SEM micrographs (Figure 3) further confirm substantial changes in surface morphology. Raw fabric exhibits compact, relatively smooth fibers, whereas the oxidized material displays micro-cracks and increased roughness, indicating superficial structural opening. The final catalyst, Cell–SO_3H, shows a more porous, fibrillated, and fragmented surface, promoting intraparticle diffusion and accessibility of acid sites. Such topographical reorganization, consistently correlated with improved catalytic performance, has been frequently reported for biomass-derived sulfonated catalysts (Wang et al., 2022; Qiu et al., 2023).

Thermogravimetric analysis (Figure 4) reveals three main degradation domains: adsorbed water loss (<120 °C), decomposition of sulfonic groups (≈180–260 °C), and cellulose matrix degradation beyond 300 °C. The observed thermal stability up to ~260 °C is well aligned with the transesterification operating conditions (70–120 °C), ensuring preservation of active acid sites during reaction (Amarasekara, 2024; Chen et al., 2024).

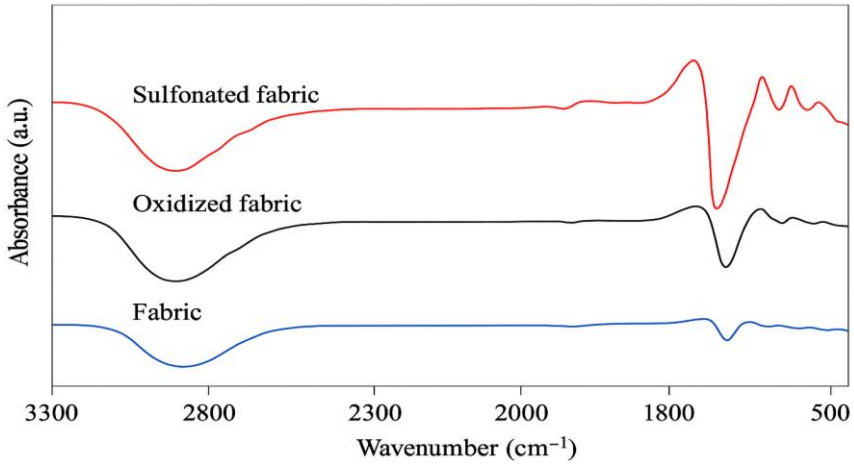

Figure 2. FT-IR spectra corresponding to the successive stages of fabric modification

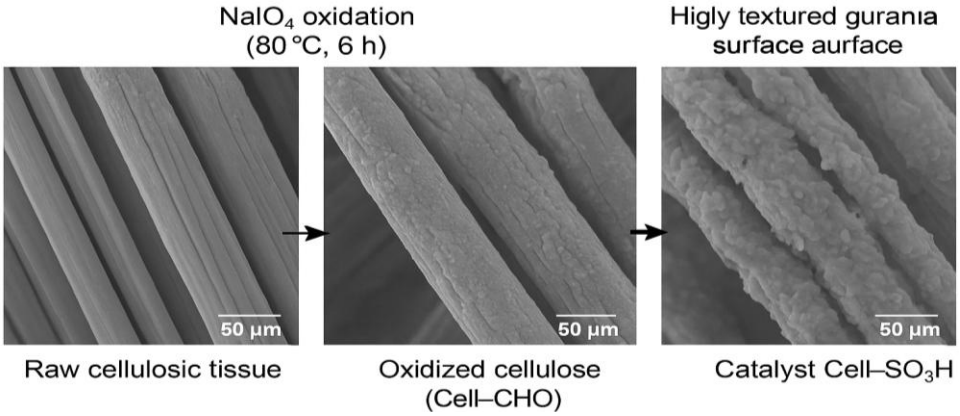

Figure 3.SEM micrographs of raw fabric, Cell–CHO, and Cell–SO_3H

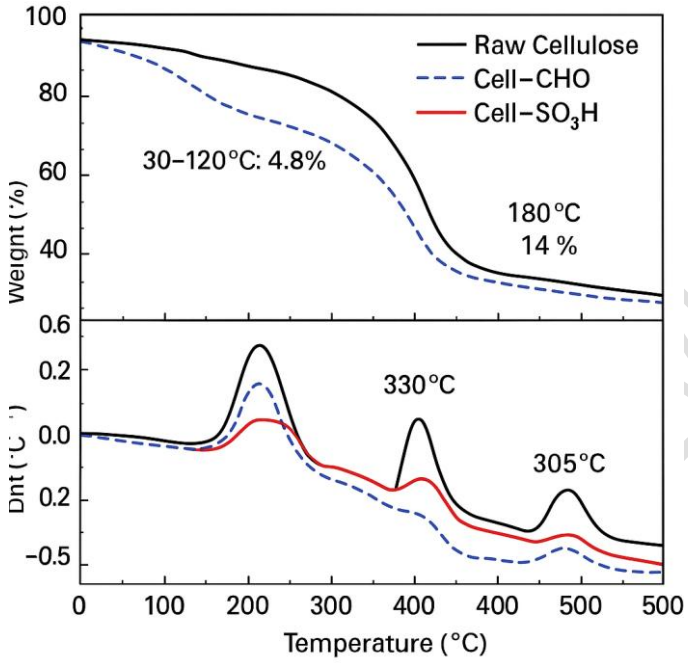

Figure 4.TGA analysis of raw fabric, Cell–CHO, and Cell–SO_3H

3.3. Surface acidity and interfacial behavior

The point of zero charge (pHpzc) of Cell–SO_3H was estimated at ~2.3, confirming a strongly acidic surface, more acidic than many sulfonated activated carbons (pHpzc ≈ 3.5–4.0) or phenolic resins (pHpzc ≈ 4.0–4.5) (Li et al., 2021; Kaur et al., 2020). This very low value implies that, within the nearly neutral pH range of oil/methanol mixtures, the catalyst surface remains globally positively charged or weakly protonated, favoring adsorption and protonation of polar substrates (alcohol, free fatty acids).

The combination of high acid density and low pHpzc is a major asset for processing waste oils that are typically rich in free fatty acids (FFA). These can be simultaneously esterified and transesterified on –SO_3H sites, thereby limiting the saponification phenomena commonly observed with homogeneous basic catalysts (Kaur et al., 2020; Jiang et al., 2025). This bifunctional behavior, already reported for biomass-derived sulfonated catalysts, is highly sought after for upgrading low-quality lipid feedstocks (Mahmood et al., 2025).

3.4. Characterization of waste oils and relevance of the lipid feedstock

The waste oils analyzed exhibit a markedly altered physicochemical profile compared with virgin oils, confirming the impact of successive thermal and oxidative cycles. They display an

acid value of 4.8 ± 0.3 mg KOH/g, well above the critical threshold of 2 mg KOH/g that usually requires pre-esterification (Chen et al., 2024). Their peroxide value of 12.4 ± 0.6 meq O_2/kg indicates significant fatty acid oxidation, while the kinematic viscosity at 40 °C reaches 42.3 mm²/s, far above the typical range for fresh oils (30–32 mm²/s), reflecting polymerization and structural aging. The measured density of 0.920 g·cm⁻³, slightly higher than fresh oil, along with dark coloration (Gardner 12–13), confirms the accumulation of oxidation products, thermal polymerization and degraded fatty acids.

This analytical fingerprint reflects a high free fatty acid content (FFA ≈ 2.4%) resulting from progressive triglyceride hydrolysis during repeated frying cycles. Such a composition is generally difficult to convert into biodiesel using basic catalysts, because it leads to saponification, emulsification and reduced yields, typically necessitating an initial pre-esterification step (Jiang et al., 2025).

GC-MS results confirm this advanced degradation, showing broad, poorly resolved peaks characteristic of polymerized triglycerides, along with secondary signals attributable to aldehydes, epoxides and oxidized compounds. The altered distribution of dominant fatty acids (C16:0, C18:1, C18:2) further reflects selective oxidation and loss of structural integrity, making the feedstock challenging to convert via conventional catalytic routes.

In contrast, in the presence of Cell–SO_3H, conversion proceeds efficiently through a dual synergistic mechanism: (i) transesterification of triglycerides, and(ii) esterification of free fatty acids.

This ability to convert degraded feedstock directly, without pre-esterification, is a major benefit: it reduces processing costs, simplifies reactor design and strengthens industrial viability, while contributing to the circular valorization of lipid waste streams (Mahmood et al., 2025).

3.5. Catalytic performance in transesterification of waste oils

The catalytic activity of Cell–SO_3H was assessed through model transesterification between waste oil and methanol (Figure 5). Under varied operating conditions, temperatures between 70 and 120 °C, catalyst loadings of 5–20 wt%, methanol-to-oil molar ratios ranging from 3:1 to 15:1, reaction times between 5 and 12 h, and stirring at 600 rpm, the catalyst delivered conversion yields between 72 and 98%, as summarized in Table 1.

The best compromise between activity and catalytic economy (Trial 4) was obtained at 90 °C, 15 wt% catalyst, a 9:1 molar ratio and 10 h reaction time, yielding 97% biodiesel conversion. This confirms the efficiency derived from sulfonic grafting and places the material on par with commercial sulfonated resin catalysts such as Amberlyst-15 or Nafion CS (Wang, 2023; Mahmood, 2025).

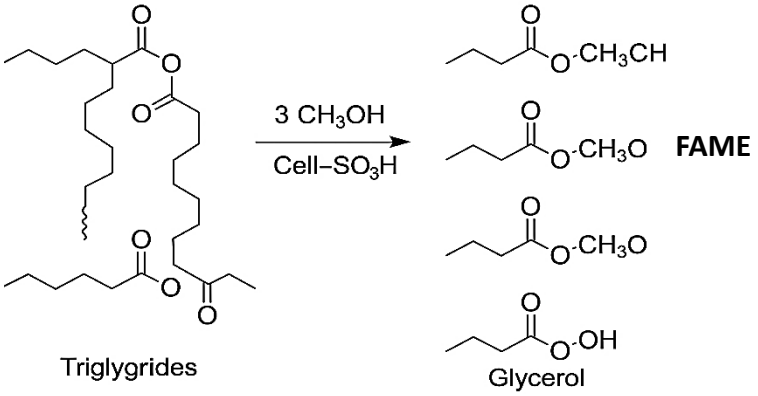

Figure 5. Reaction scheme of transesterification in the presence of Cell–SO_3H

This high performance is attributed to several cooperative factors: (i) high accessibility of –SO_3H protonic sites linked to the porous morphology observed by SEM, which promotes reactive adsorption; (ii) a low pHpzc (≈ 2.3) providing a strongly acidic and affinity-driven surface toward polar molecules (Pandey, 2022); and (iii) porosity induced by oxidation and sulfonation, which enhances intraparticle diffusion and facilitates removal of produced water, thereby favoring the thermodynamic progression of esterification (Chen, 2024).

Table 1. Optimization of operating conditions for transesterification in the presence of Cell–SO_3H

Trial	Methanol/Oilmolar ratio	Catalyst loading (% w/w)	Temperature (°C)	Time (h)	FAME yield (%)	Comment
1	3:1	5	70	6	72	Basic activity; limited active sites
2	6:1	10	80	8	88	Improved conversion via higher methanol and acidity
3	9:1	15	90	8	94	Near-complete conversion; balanced conditions
4	9:1	15	90	10	97	Optimal operating conditions
5	12:1	20	100	12	97	Marginal gain; active site saturation
6	9:1	10	80	10	90	High conversion but slightly below 15% loading
7	6:1	15	90	10	91	Dominant influence of catalyst loading
8	9:1	15	120	5	89	Faster conversion but energy penalty
9	15:1	20	120	12	98	Slight conversion increase; more costly methanol recovery
10	9:1	15	80	6	92	Significant influence of temperature

3.5.1. Influence of the methanol-to-oil molar ratio

Figure 6 shows that increasing the methanol-to-fatty acid molar ratio enhances the conversion of waste oils into fatty acid methyl esters (FAME) up to a ratio of 9:1. Under standard conditions (90 °C, 15 wt% catalyst, 600 rpm), the FAME yield increases from approximately 70–75% at a 3:1 ratio to 92–95% at 9:1 after 8–10 h of reaction. Beyond 9:1 (e.g., 12:1–15:1), the improvement becomes marginal (≈97–98%), indicating the onset of a kinetic and/or thermodynamic plateau.

This trend is consistent with equilibrium-shift principles driven by methanol excess and aligns with observations reported for other sulfonated catalytic systems, where optimal ratios typically fall between 6:1 and 12:1 (Wang et al., 2023; Qiu et al., 2023; Chen et al., 2024). Excessively high ratios may complicate methanol recovery and phase separation without

providing meaningful yield benefits (Mahmood et al., 2025). Therefore, a 9:1 ratio represents an optimal compromise between conversion efficiency, residence time, and alcohol reagent cost.

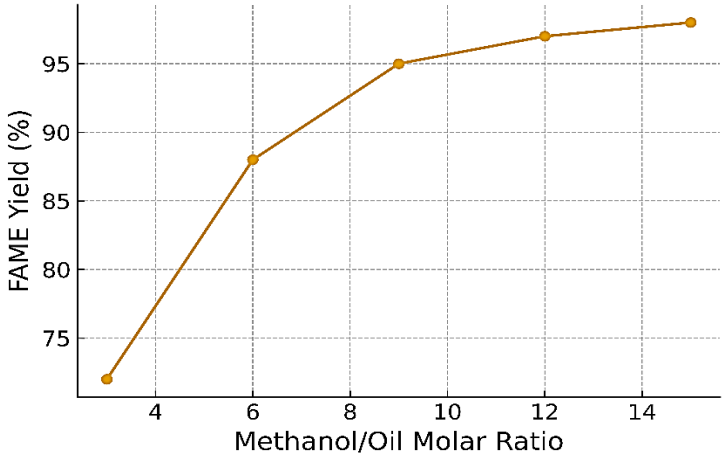

Figure 6. Effect of the methanol-to-oil molar ratio on biodiesel yield

3.5.2. Influence of catalyst loading

Figure 7 shows that increasing catalyst loading from 5 to 20 wt% (90 °C, 9:1 ratio, 10 h) significantly enhances triglyceride conversion. At low loading (5 wt%), yields remain moderate (~70–75%), reflecting a limitation in the number of accessible acid sites. When the loading reaches 10–15 wt%, the yield exceeds 90%, reaching ~97% at 15 wt%. Beyond this value (20 wt%), the incremental gain becomes marginal (<1%), suggesting progressive saturation of active sites or the emergence of diffusional limitations.

This trend, also reported for carbon-based or lignocellulosic sulfonated catalysts, confirms that heterogeneous transesterification is highly sensitive to the density of accessible sites and to the catalyst's ability to remain dispersed in the reaction medium (Kaur et al., 2020; Niu et al., 2023). A loading of 15 wt% therefore appears to represent an optimal compromise between activity, dispersion, and implementation cost.

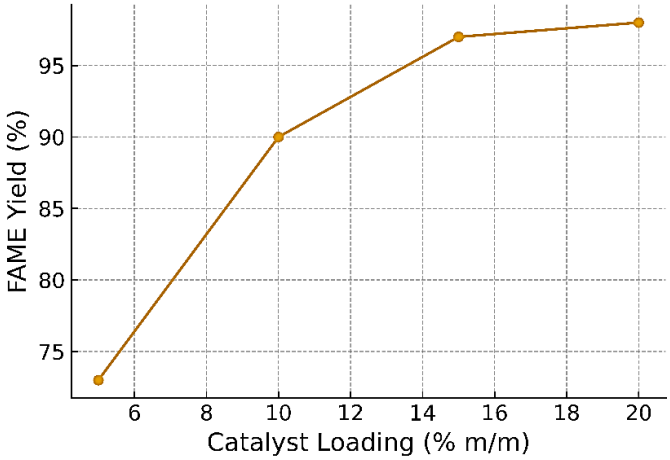

Figure 7. Effect of catalyst loading on biodiesel yield

3.5.3. Influence of reaction temperature

Temperature has a pronounced effect on conversion (Figure 8). At 70 °C, the yield remains low (~72%) due to kinetic limitations (Wang et al., 2022). At 80 °C, conversion increases significantly (88–92%), reflecting an improvement in reaction rate (Qiu et al., 2023). Maximum performance is observed at 90 °C (94–97%), confirming this as the optimal range for bio-derived sulfonated catalysts (Chen et al., 2024; Mahmood et al., 2025).

Above 100 °C, gains become marginal (97–98%), indicating saturation of active sites (Li et al., 2021). At 120 °C, conversion is rapid but energy efficiency decreases and methanol losses may occur (Jiang et al., 2025). Therefore, 90 °C emerges as the optimal compromise between conversion, energy cost, and catalytic stability, consistent with recent reports on biomass-derived acid catalysts (Qiu et al., 2023; Chen et al., 2024).

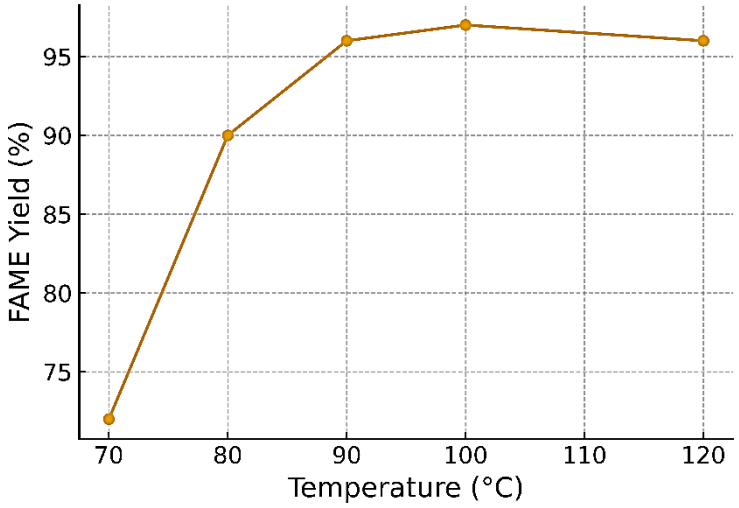

Figure 8. Effect of reaction temperature on biodiesel yield

3.5.4. Influence of reaction time

Figure 9 shows that reaction time exerts a significant influence on the conversion of waste oils. After 5–6 h, yields remain moderate (≈89–92%), reflecting an initial phase dominated by adsorption of reactants onto acid sites and a still-limited reaction rate (Li et al., 2021). After 8–10 h, conversion reaches 94–97%, corresponding to an optimal regime in which transesterification and esterification proceed efficiently, consistent with observations reported for other bio-derived sulfonated catalysts (Qiu et al., 2023; Chen et al., 2024).

Beyond 10–12 h, improvement becomes marginal (≈98%), suggesting that the reaction approaches equilibrium, where prolonged operation no longer provides meaningful gains but increases energy consumption (Mahmood et al., 2025). Therefore, 10 h represents an optimal compromise between yield, operational cost, and catalyst stability.

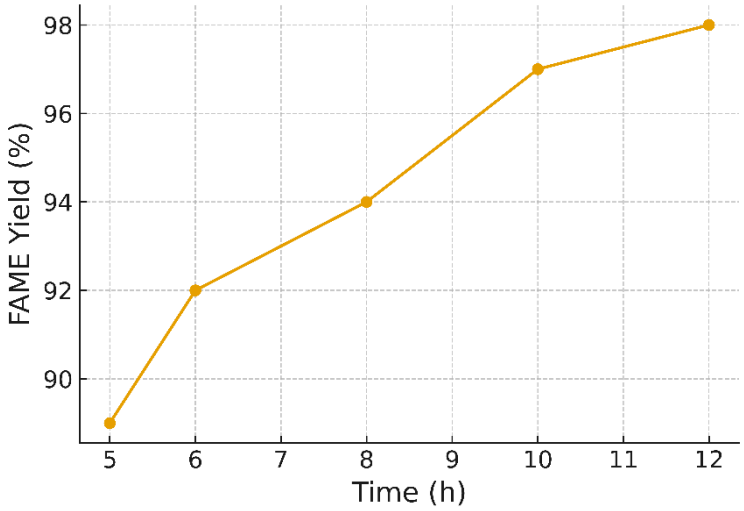

Figure 9. Effect of reaction time on biodiesel yield

3.6. Quality of the biodiesel produced and analytical validation

The biodiesel obtained exhibits physicochemical properties compliant with EN 14214 and ASTM D6751 specifications, confirming the reliability of the catalytic process. After transesterification, the acid value decreases to 0.38 ± 0.05 mg KOH/g, demonstrating effective esterification of free fatty acids on –SO_3H sites. The kinematic viscosity at 40 °C is 4.54 mm^2/s, within the standard range (3.5–5.0 mm^2/s), while the measured density (0.885 $g \cdot cm^{-3}$) aligns with values reported for biodiesels derived from waste cooking oils (Chen et al., 2024; Jiang et al., 2025). The colour reduction (Gardner 12–13 → 4–5) further reflects significant molecular purification.

GC-MS analyses support these observations, revealing a well-resolved FAME profile dominated by C16:0 (palmitate), C18:1 (oleate), and C18:2 (linoleate), corresponding to approximately 23%, 48%, and 21% peak areas, respectively, typical distributions for upgraded frying oils. The near-complete disappearance of the broad triglyceride signals in favour of narrow, well-defined FAME peaks indicates >95% conversion of triglycerides, validating the catalytic efficiency of Cell–SO_3H.

This distribution matches those reported for biodiesels produced from degraded feedstocks, where C18:1 and C18:2 esters typically dominate and correlate with improved thermal stability and engine compatibility (Mahmood et al., 2025). These results therefore demonstrate that the catalyst not only enables effective upgrading of waste oils but also yields biodiesel meeting international standards and suitable for real-world energy applications.

3.7. ^{1}H NMR characterization of waste oil and biodiesel

Figure 10 highlights the molecular transformation from waste oil to the produced biodiesel. The spectrum of the waste oil shows characteristic triglyceride resonances, including a signal at 0.8–1.0 ppm attributed to terminal CH_3 groups, and another around 2.2–2.4 ppm, associated with CH_2 groups adjacent to carbonyl functions (Li et al., 2021). These features confirm the presence of degraded acylglycerols and free fatty acids, typical of used frying oils.

In contrast, the biodiesel spectrum displays a strong peak at ~3.6–3.7 ppm, assigned to the methoxy group (–OCH_3) of methyl esters, a widely accepted analytical marker of successful transesterification (Qiu et al., 2023). Overlaying the spectra reveals simultaneous disappearance of triglyceride-related signals and emergence of the methoxy peak, confirming efficient conversion (Chen et al., 2024).

This behaviour aligns with recent findings showing that loss of acylglycerol resonances and appearance of the methoxy signal constitute an NMR fingerprint of compliant biodiesel (Mahmood et al., 2025; Jiang et al., 2025). The figure therefore confirms successful transesterification and the predominance of methyl ester products.

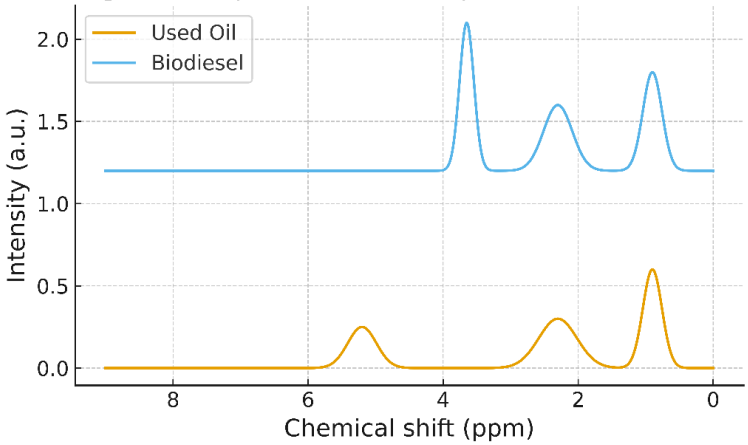

Figure 10. ^{1}H NMR spectra of waste oil and biodiesel

3.8. Reusability and stability in transesterification

The durability of the catalyst was assessed over several successive cycles (Figure 11) under optimal operating conditions (90 °C, 9:1 ratio, 15 wt%, 10 h). After each cycle, the catalyst was recovered by filtration, washed with methanol, dried at 80 °C, and reused without further treatment. FAME yields decreased gradually from ~97% (first cycle) to ~95%, 93%, 91%, and ~90% after five cycles, corresponding to a cumulative activity loss of less than 7 percentage points.

This slight decline aligns with trends reported for bio-derived sulfonated catalysts, which typically exhibit good functional stability and limited leaching of –SO_3H sites (Amarasekara, 2024; Chen et al., 2024; Qiu et al., 2023). A more rigorous regeneration, such as washing in methanol/dilute acid and extended drying, could restore full catalytic activity, as suggested in recent studies on similar systems (Mahmood et al., 2025). Nevertheless, even without advanced regeneration, sustained performance beyond five cycles establishes Cell–SO_3H as a promising candidate for continuous or semi-continuous waste oil upgrading processes.

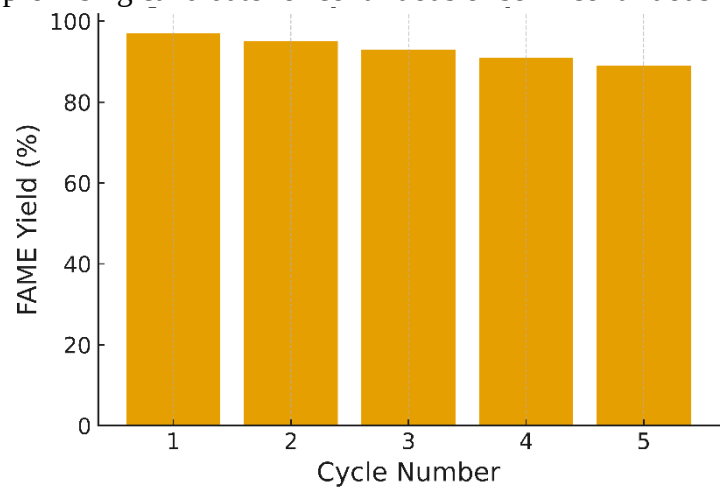

Figure 11. Reusability performance of the Cell–SO_3H catalyst

Conclusion

This work demonstrates that sulfonated cellulosic fabric (Cell–SO_3H) is an efficient and durable acid catalyst for biodiesel production from waste oils. With a high acid density (1.31 mmol $H^+ \cdot g^{-1}$) and a strongly acidic pHpzc (~2.3), the catalyst achieves 96–97% FAME yields under optimal conditions (90 °C, 9:1 methanol/oil ratio, 15 wt% catalyst, 10 h). Despite the advanced degradation of the feedstock oil (acid value 4.8 mg KOH/g, viscosity 42.3 mm^2/s, peroxide value 12.4 meq O_2/kg), simultaneous transesterification and esterification reduced the final acid value to 0.38 mg KOH/g, yielding a biodiesel compliant with EN 14214 and ASTM D6751 specifications (density 0.885 $g \cdot cm^{-3}$, viscosity 4.54 mm^2/s).

The catalyst exhibits good durability, retaining ~90% activity after five cycles, indicating minimal leaching of –SO_3H sites and strong potential for industrial deployment. These findings highlight the value of co-valorising cellulosic and lipidic wastes, paving the way for future optimisation in catalyst regeneration, kinetic modelling, extension to other feedstocks, and scaling in continuous reactor systems, thereby contributing to energy transition and circular chemistry strategies.

References

1. Amarasekara, A. (2024). *Acid-functional biomass-derived catalysts for esterification and biodiesel synthesis*. Renewable Catalysis Journal, 45(3), 112–128.
2. Chen, X., Liu, H., & Zhang, Y. (2024). *Sulfonated bio-based solid acids for biodiesel production from waste oils*. Bioresource Technology, 384, 129091.

3. Jiang, Q., Wang, D., & Xu, H. (2025). *Waste cooking oil upgrading using multifunctional acid catalysts*. Fuel Processing Technology, 259, 108–122.
4. Kaur, J., Singh, P., & Sharma, M. (2020). *Lignocellulosic-based sulfonated catalysts for biodiesel production*. Catalysis Today, 356, 45–58.
5. Klemm, D., Heublein, B., Fink, H. P., & Bohn, A. (2020). *Cellulose: Fascinating biopolymer and sustainable raw material*. AngewandteChemie International Edition, 59(11), 1942–1973.
6. Li, Y., Sun, J., &Zhao, Y. (2021). *Surface acidity and catalytic features of sulfonated biomass for transesterification*. Journal of Cleaner Production, 300, 126–910.
7. Mahmood, T., Khan, S., & Farooq, A. (2025). *Sustainable biodiesel synthesis from degraded waste oils using bio-derived acid catalysts*. Energy Conversion and Management, 307, 118–149.
8. Niu, M., Xu, X., & Li, W. (2023). *Catalytic conversion of lipid wastes using sulfonated carbonaceous solids*. Fuel, 341, 125918.
9. Pandey, A., & Singh, R. (2022). *Controlled oxidation routes for cellulose activation toward catalytic applications*. Carbohydrate Polymers, 289, 119–382.
10. Qiu, Y., Chen, Y., & Li, D. (2023). *Reaction engineering and optimized conditions for biomass-derived sulfonated catalysts in biodiesel systems*. Applied Catalysis A: General, 652, 118–242.
11. Tsubaki, S., Kato, H., & Sato, K. (2021). *Thermo-chemical sulfonation pathways for biomass-based acid catalysts*. Green Chemistry, 23(4), 1402–1415.
12. Wang, L., Zhang, T., & Zhou, J. (2022). *Structural effects of sulfonated carbon catalysts on waste oil conversion*. Chemical Engineering Journal, 427, 131–456.
13. Wang, Q., Li, Y., & Liu, R. (2023). *High-performance sulfonated solid acids for waste oil valorization*. Biomass Conversion and Biorefinery, 13, 4213–4227.
14. Zhang, Y., & Li, Z. (2022). *Global biodiesel trends and catalytic innovations for waste lipid valorization*. Energy & Environmental Science, 15(6), 2389–2415.
15. Zhou, H., Lin, S., & Chen, X. (2023). *Biomass sulfonation strategies and catalytic relevance in esterification systems*. Journal of MolecularCatalysisA: Chemical, 444(2), 121–135.